LASER INTERFEROMETER GRAVITATIONAL WAVE OBSERVATORY
-LIGO-
CALIFORNIA INSTITUTE OF TECHNOLOGY
MASSACHUSSETTS INSTITUTE OF TECHNOLOGY

Technical Note **LIGO-T010038- 00- Z** 3/20/01

E2 Correlations

Nelson Christensen, Tom Robinson
Physics and Astronomy, Carleton College,
Northfield, MN 55057 USA

Adrian Ottewill
Department of Mathematical Physics, University College Dublin,
Belfield, Dublin 4, Ireland

This is an internal working note
of the LIGO Project.

California Institute of Technology
LIGO Project - MS 51-33
Pasadena CA 91125
Phone (818) 395-2129
Fax (818) 304-9834
E-mail: info@ligo.caltech.edu

Massachusetts Institute of Technology
LIGO Project - MS 20B-145
Cambridge, MA 01239
Phone (617) 253-4824
Fax (617) 253-7014
E-mail: info@ligo.mit.edu

WWW: http://www.ligo.caltech.edu/

file correlation.tex- printed March 22, 2001

1 Introduction

It was the goal of this group to quantify correlations between various interferometer control and environmental channels. This present study of the E2 data attempts to identify sources of noise in the interferometer output. As the interferometer noise from the E2 run was approximately five orders of magnitude larger than the desired noise level it is apparent that this study will presently be only marginally useful. Still, it is informative to see where the correlations are. Other systems were behaving relatively well, and we can see where environmental noise was corrupting operation. Results are presented for investigations of the mode cleaner, the pre-mode cleaner, the pre-stabilized laser and other systems.

1.1 Method

A detailed description of the DMT code used for this study can be found elsewhere [1, 2]. The method implemented here works by estimating the linear transfer function between the principal channel and specified environmental channels on the basis of the correlations over a certain bandwidth in Fourier space. We denote the channel of interest by X or Y_1. The other sampled channels consist of environmental and instrumental monitors which we denote $Y_2, \ldots, Y_N$. The channels are decimated so that all channels are sampled at the slowest rate of any channel $Y_1, \ldots, Y_N$.

We assume that the contribution of channel i to channel 1 is described by an unknown linear transfer function $R_i(t-t')$. The basic idea of the method is to use the data to estimate the transfer functions R_i. We work with the data in Fourier space. The transfer function is estimated by averaging over a frequency band, that is a given number of frequency bins. The number of bins in any band is denoted by F in [2] and `correlationWidth` in the associated programs [1]. The method assumes that $\tilde{R}_i$ can be well approximated by a *complex constant* within each frequency band, in other words that the transfer function does not vary rapidly over the frequency bandwidth $\Delta f = F/T$ where T is total time of the data section under consideration. The choices 32, 64 and 128 appear most appropriate for F, and we used 64 for this present study. Given that we analyzed data in 8s and 64s sections this corresponds to averaging over frequency spans of 8Hz and 1Hz spans respectively. Within a given band, b, the Fourier components of the field may be thought of as the components of a complex F-dimensional vector, $\mathbf{Y}_i^{(b)}$. The correlation between two channels (or the auto-correlation of a channel with itself) may be expressed by the standard inner product $(\mathbf{Y}_i^{(b)}, \mathbf{Y}_j^{(b)}) = \mathbf{Y}_i^{(b)} \cdot \mathbf{Y}_j^{(b)*}$:

$$\rho_i^{(b)} = \frac{\left|(\mathbf{X}^{(b)}, \mathbf{Y}_i^{(b)})\right|}{\left|\mathbf{X}^{(b)}\right|\left|\mathbf{Y}_i^{(b)}\right|}.$$

The limits are $0 \leq \rho_i^{(b)} \leq 1$. For the timescales used in this study values of $\rho_i^{(b)} \lesssim 0.2$ are not statistically significant, while strong correlations correspond to $\rho_i^{(b)} \gtrsim 0.75$. The figures in this document display $\rho_i^{(b)}$ on a scales from 0 to 1 (top display) and 0.75 to 1 (bottom display).

The DMT code provides the ability to 'clean' the principal channel on the basis of the determined correlations with environmental channels. We decided that the E2 data did not justify such an investigation but we plan to conduct such a 'cleaning' for future engineering runs.

1.2 E2 Data

We looked at various sections of data when the recombined interferometer was locked during the E2 run. In addition, we ensured that the data used was in fact good by examining the time series of H2:LSC-AS_Q, H2:LSC-AS_I, H2:LSC-LA_NPTRR, H2:LSC-LA_NPTRT, plus the power density of H2:LSC-AS_Q.

We attempted to see if we could observe some indication for the loss of interferometer lock. Hence we examined two types of data; (1) one set was in the middle of a long ($> 1000s$) section of locked interferometer operation, (2) while the other set was within a minute of lock loss. The data for type (1) (interferometer locked and working well) can be found on `stone` in /export/raid3/E2/ and stated with the first frame file in the directories of 00-11-09_09:17:47.5, 00-11-09_09:17:47.40, 00-11-09_09:17:47.63, 00-11-08_19:59:35.4. For data from set (2) (approximately a minute before the interferometer lost lock) we looked at 00-11-08_19:59:35.11/H-657789150.F, 00-11-08_19:59:35.11/H-657789000.F, 00-11-09_09:17:47.74/H-658063730.F, and 00-11-09_09:17:47.74/H-658063600.F. There were no apparent increases or changes in correlations that could be attributed to lock-loss. The data was analyzed in either 8 s or 64 s sections.

In this report we will show typical correlations observed. Numerous other examples, and all of our results can be found on the WWW:

`http://physics.carleton.edu/Faculty/res67/E2corr.htm`.

It should be noted that many of the observed correlations are to be expected. As an example, the mode cleaner mixer output (H2:IOO-MC_I) and the interferometer arm control signal (H2:LSC-CARM_CTRL) are derived from the error signal H2:LSC-AS_I. Similarly, the correlations observed between the interferometer output H2:LSC-AS_Q and the suspension channels, which can be seen in Figs. 6 and 7 below, are to be expected since they are measuring similar quantities.

During the E2 run the digital phase adjustment mixed I and Q phases at the level of 15 to 20%. Considering the overall quality of the data, it was decided that there was not a lot to be gained by correcting the phase. Correlations from this phase error can be seen in Figs. 1 and 2.

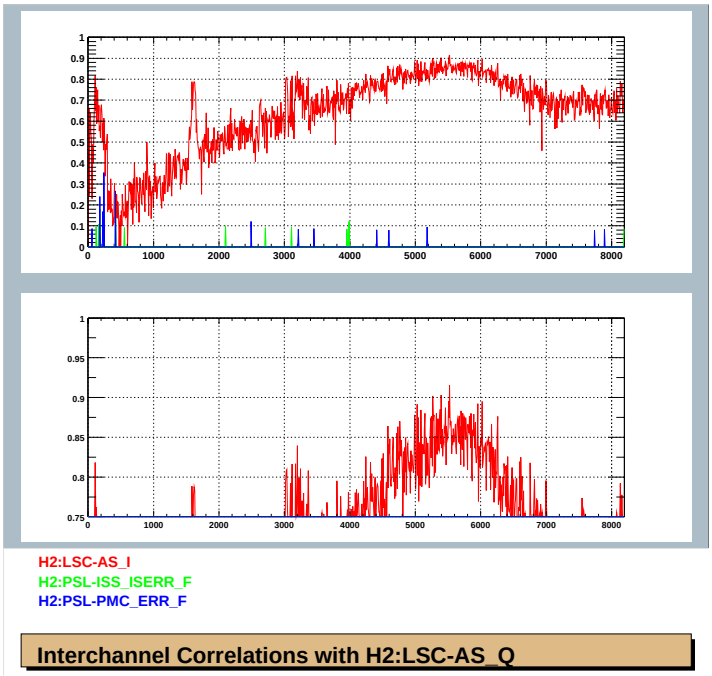

Figure 1: The correlation between H2:LSC-AS_Q and H2:LSC-AS_I.

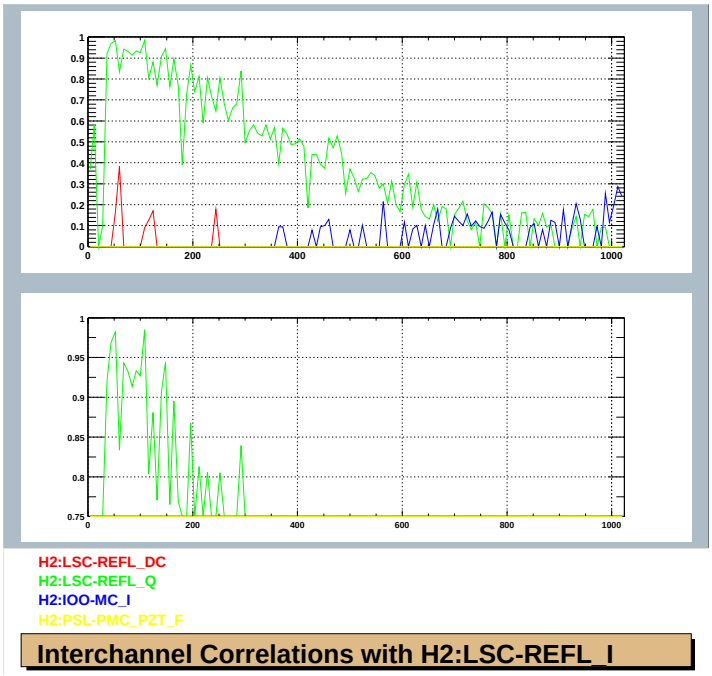

Figure 2: The correlation between H2:LSC-REFL_I and H2:LSC-REFL_Q.

2 H2:LSC-AS_Q

The interferometer output is the main location for which it is important to reduce noise. The correlation of H2:LSC-AS_Q was computed for numerous environmental and control channels. There were many interesting correlations with control channels, and those will be presented in their own sections below.

For the environmental channels there was much to be seen. There were some pronounced lines to be seen with accelerometers, with a typical observation seen in Fig. 3.

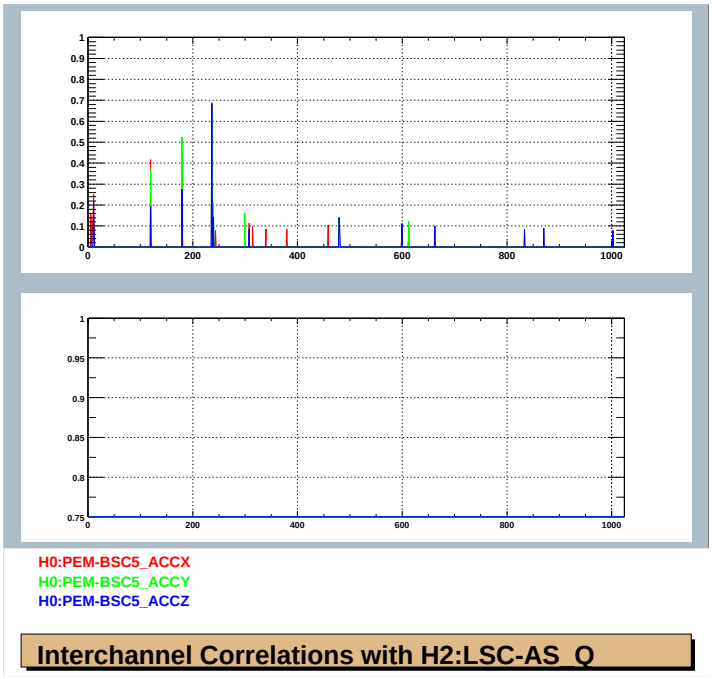

Figure 3: Typical correlation between H2:LSC-AS_Q and accelerometers.

Correlation with seismometers can be seen in Fig. 4. All seismometers showed a strong and consistent correlation just below 120 Hz, but not 60 Hz correlation was observed. Strong correlations could be seen below 20 Hz.

The tilt meter correlations did not show much of interest, while the voltage monitors correlations displayed 60 Hz and harmonics. The microphones did register correlated signals, as can be seen Fig. 5. However note that many of these spikes are at 60 Hz or harmonics.

Strong correlations are also apparent with the suspension channels at low (Fig. 6) and high (Fig. 7) frequencies.

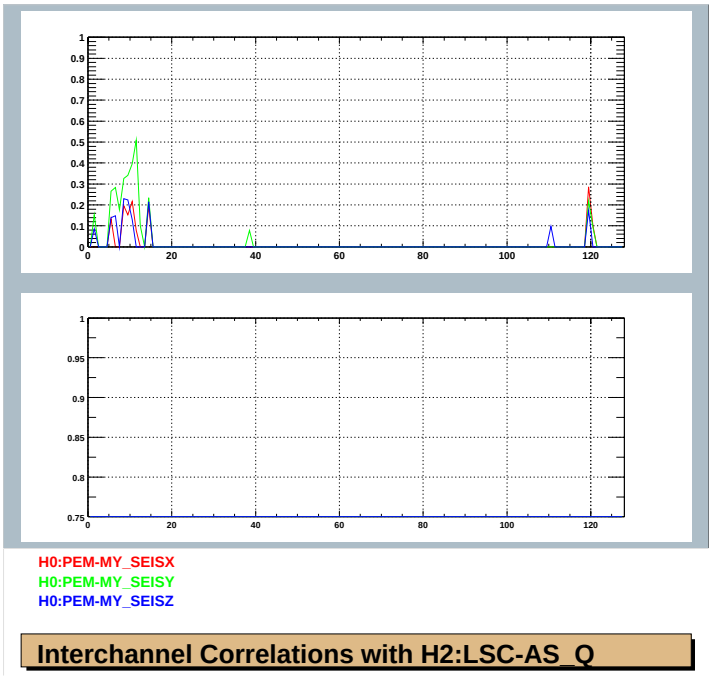

Figure 4: Typical correlation between H2:LSC-AS_Q and some seismometers.

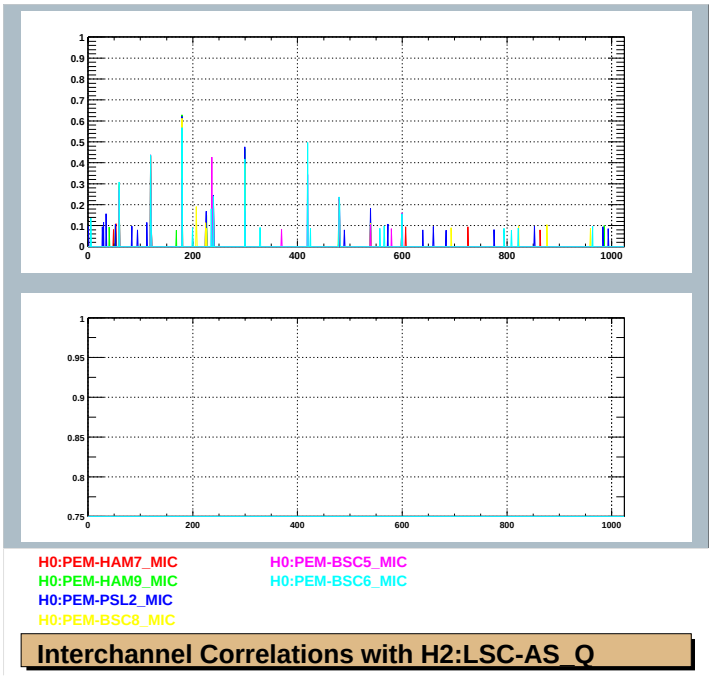

Figure 5: Correlations between H2:LSC-AS_Q and microphones.

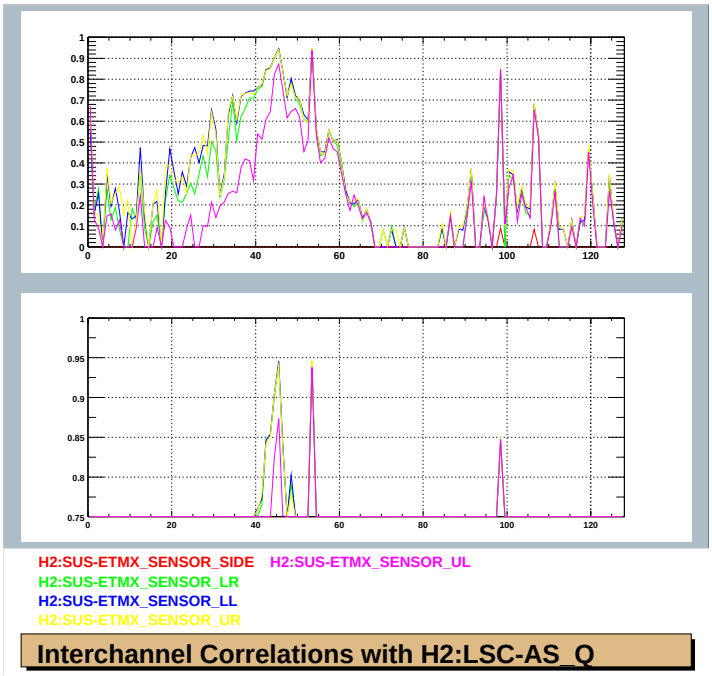

Figure 6: Low frequency correlations between H2:LSC-AS_Q and suspension channels.

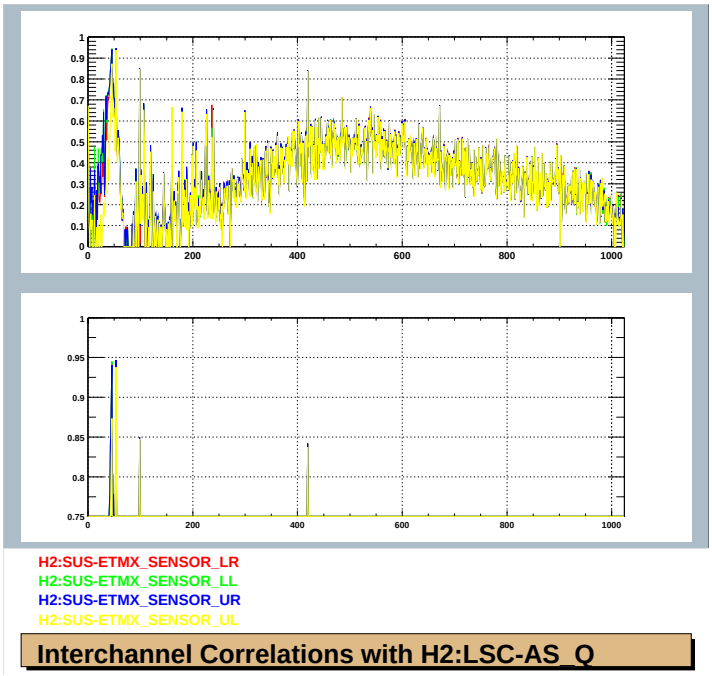

Figure 7: High frequency correlations between H2:LSC-AS_Q and suspension channels.

3 Mode Cleaner

The mode cleaner is a source of many correlations with the interferometer output. A good example can be seen in Fig. 8 (high frequency) where there are numerous correlations between H2:LSC-AS_Q and H2:IOO-MC_F from 0 - 300 Hz.

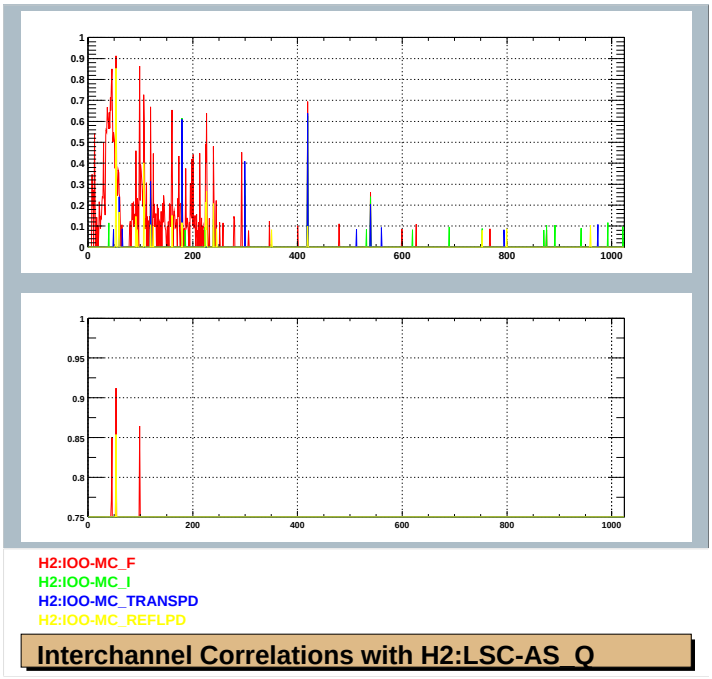

Figure 8: High frequency correlations between H2:LSC-AS_Q and mode cleaner channels.

In Fig. 9 we can see further mode cleaner correlations with H2:LSC-AS_Q and H2:IOO-MC_F, H2:IOO-MC_L and H2:IOO-MC_REFLPD up through 128 Hz.

The mode cleaner signal H2:IOO-MC_F was correlated with some control signals and environmental channels. There are numerous correlations to be seen with the accelerometers, see Figs. 10 and 11.

There are also plenty of correlations to be seen with various microphones; see Fig. 11.

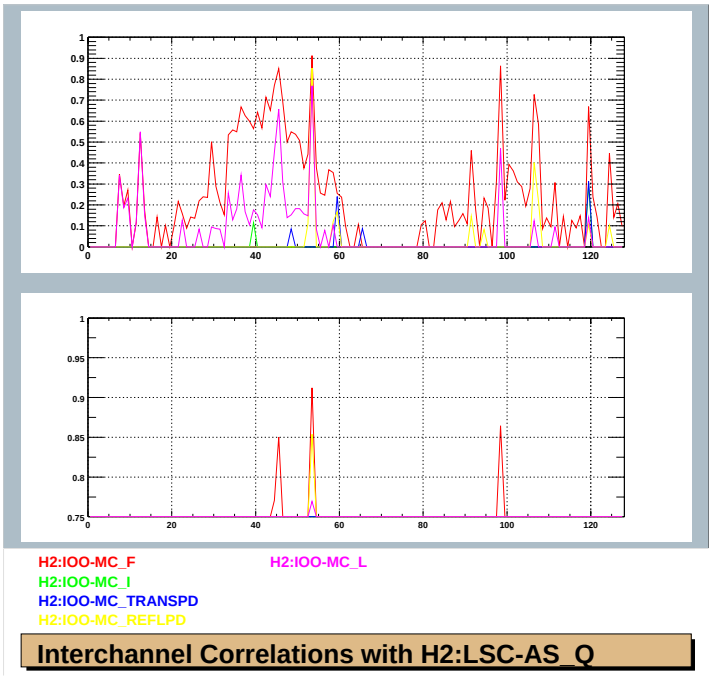

Figure 9: Correlation of interferometer output H2:LSC-AS_Q with Mode Cleaner channels.

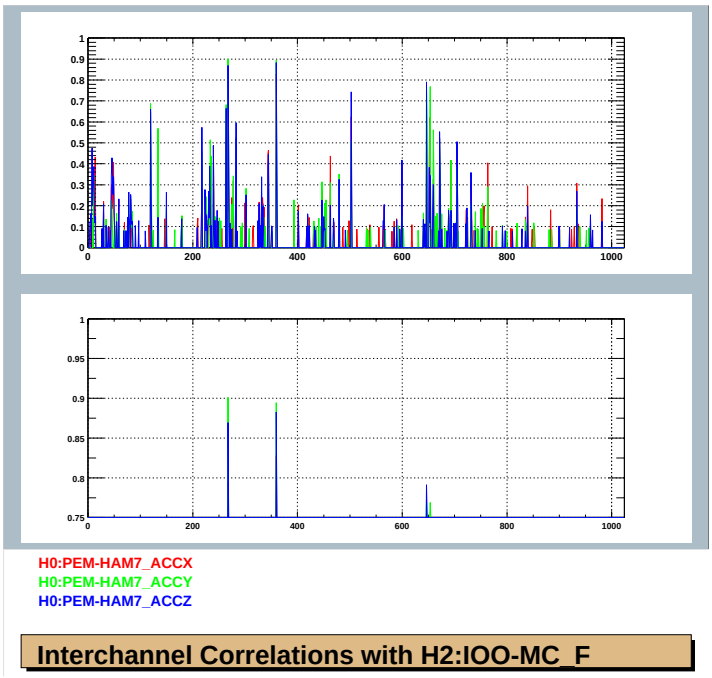

Figure 10: Correlations between mode cleaner mixer output H2:IOO-MC_F and the HAM7 accelerometers.

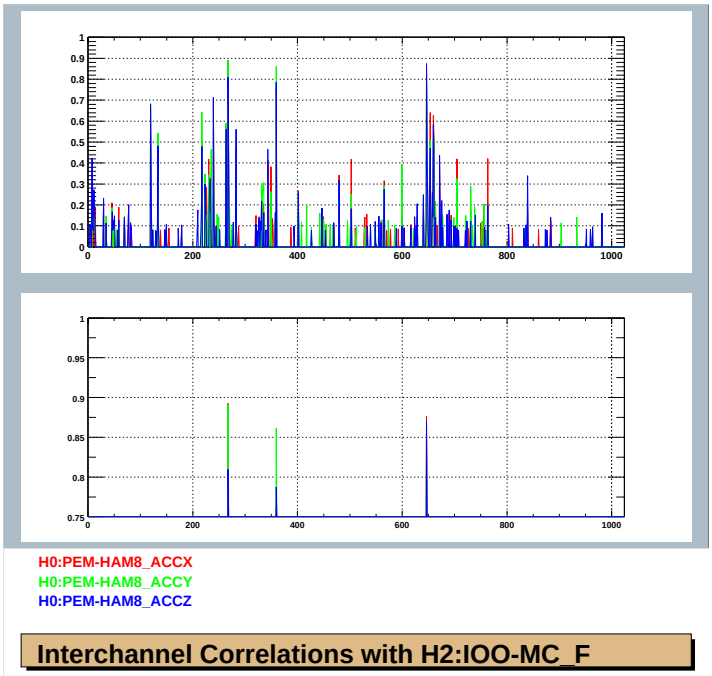

Figure 11: Correlations between mode cleaner mixer output H2:IOO-MC_F and HAM8 accelerometers.

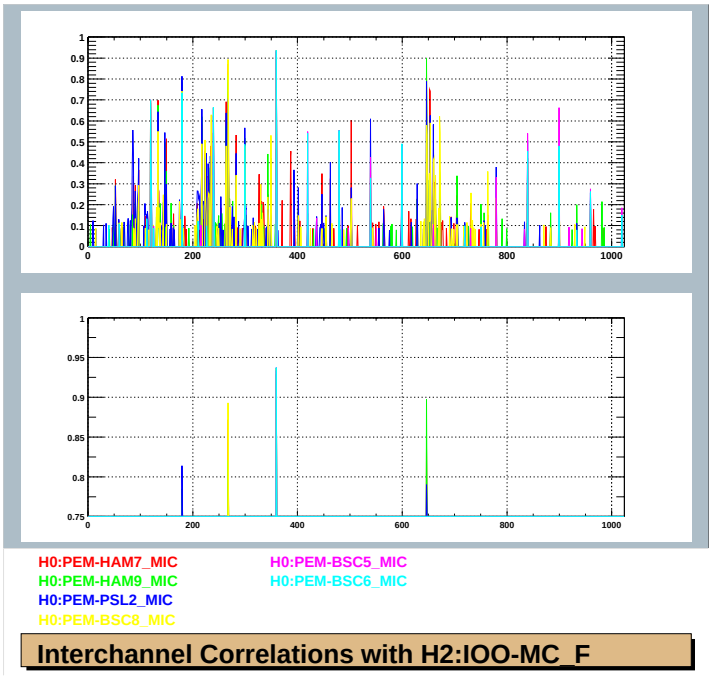

Figure 12: Correlations between mode cleaner mixer output H2:IOO-MC_F and various microphones.

4 Pre-Mode Cleaner H2:PSL-PMC_ERR_F

Correlations between the pre-mode cleaner signal, H2:PSL-PMC_ERR_F and the interferometer output H2:LSC-AS_Q were mainly observed at 60 Hz and harmonics; see Fig. 13.

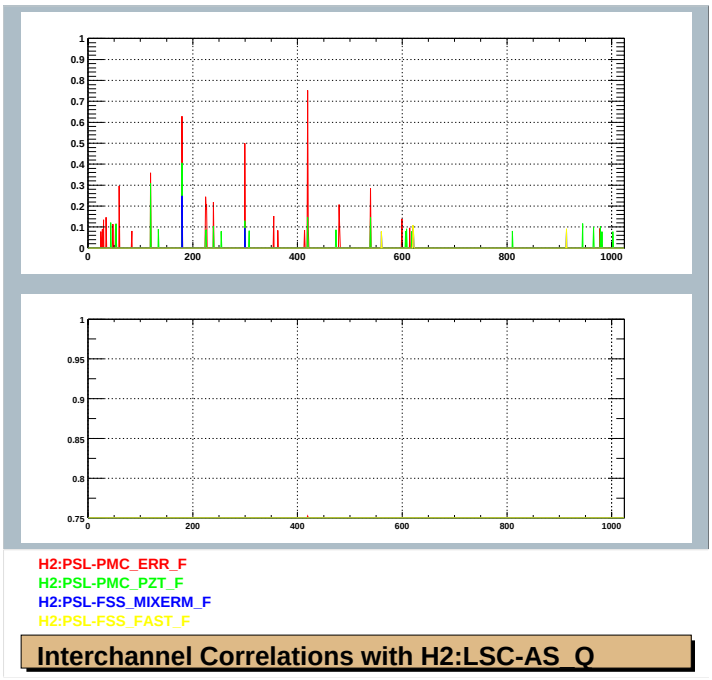

Figure 13: The pre-mode cleaner signal H2:PSL-PMC_ERR_F was correlated with the interferometer output H2:LSC-AS_Q.

The channel was also correlated with environmental monitors, and appeared to be highly correlated with its environment. Numerous correlations were observed with various microphones; see Fig. 14.

There was also much correlation to be seen with the accelerometers; see Figs. 15 and 16.

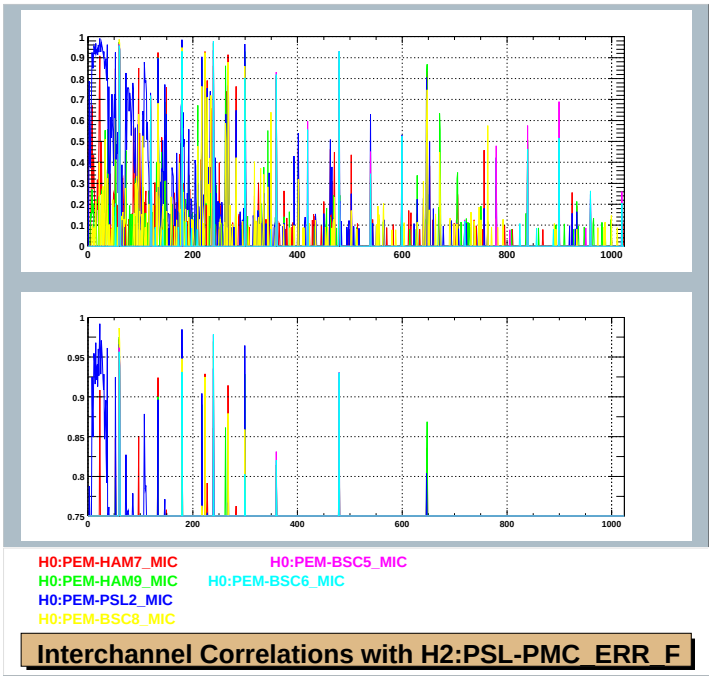

Figure 14: The pre-mode cleaner signal H2:PSL-PMC_ERR_F with observed correlations with numerous microphone channels.

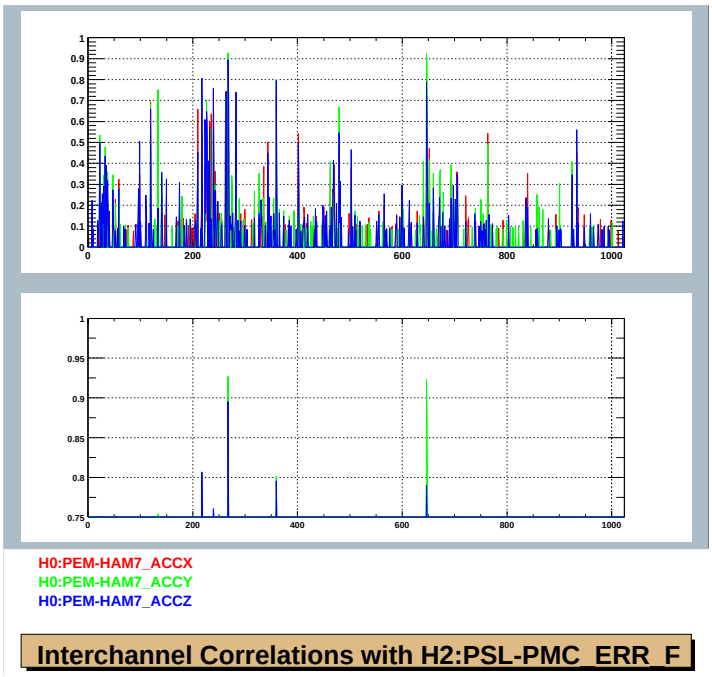

Figure 15: The pre-mode cleaner channel H2:PSL-PMC_ERR_F was found to be highly correlated with the HAM7 accelerometers.

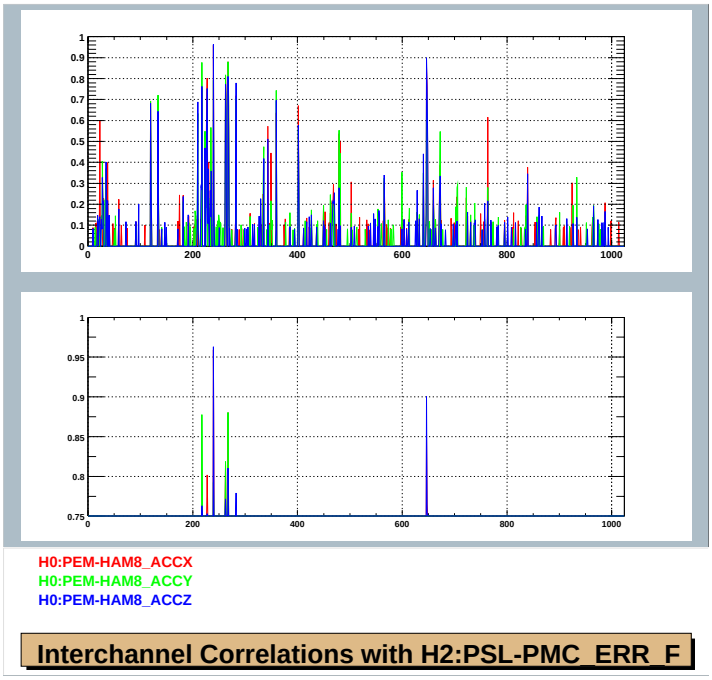

Figure 16: The pre-mode cleaner channel H2:PSL-PMC_ERR_F was found to be highly correlated with the HAM8 accelerometers.

5 H2:PSL-FSS_FAST_F

The fast feedback frequency control signal, H2:PSL-FSS_FAST_F, was not observed to be correlated with the interferometer output H2:LSC-AS_Q; see Fig. 17.

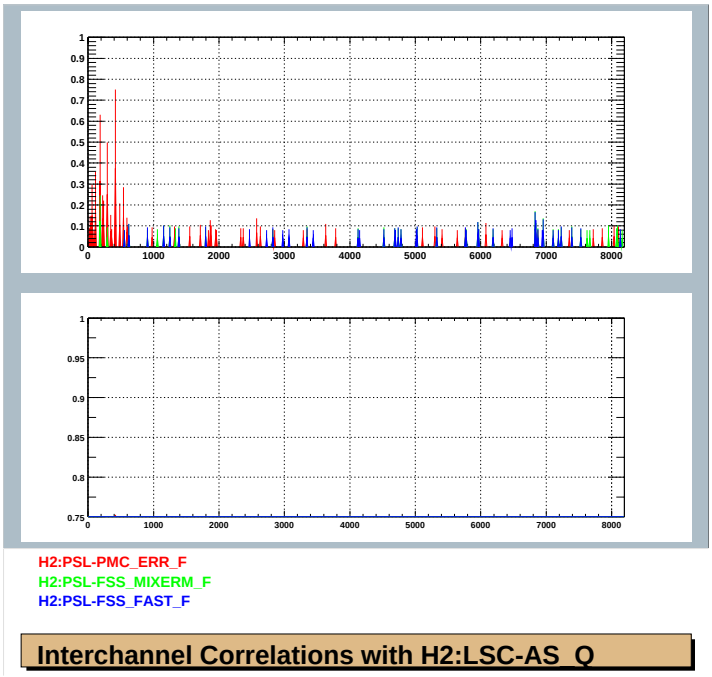

Figure 17: The laser's fast frequency control signal, H2:PSL-FSS_FAST_F, was only observed to have small correlations with the interferometer output, H2:LSC-AS_Q. These appeared at relatively high frequencies.

There were just assorted small correlations to be found with the microphones; see Fig. 18. Insignificant correlations were observed with accelerometers; see Fig. 19.

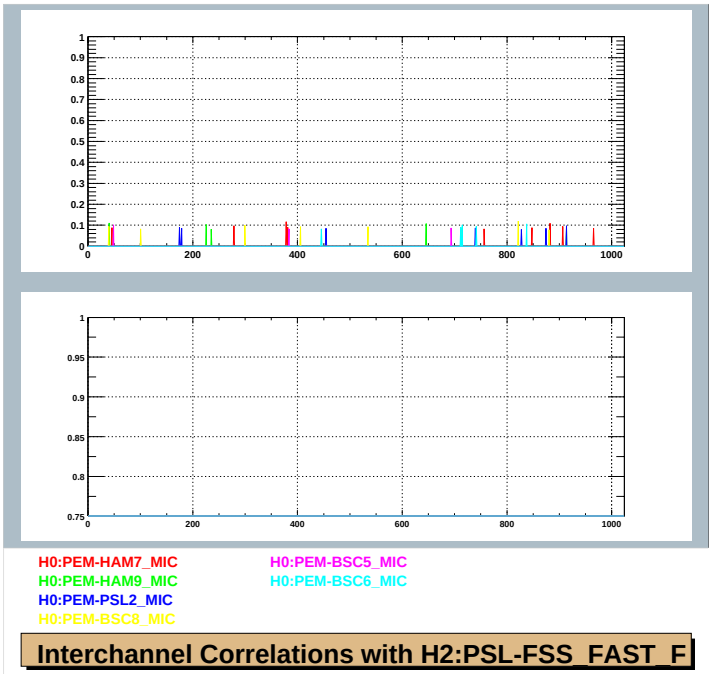

Figure 18: Correlations between laser fast frequency control signal, H2:PSL-FSS_FAST_F, and various microphones.

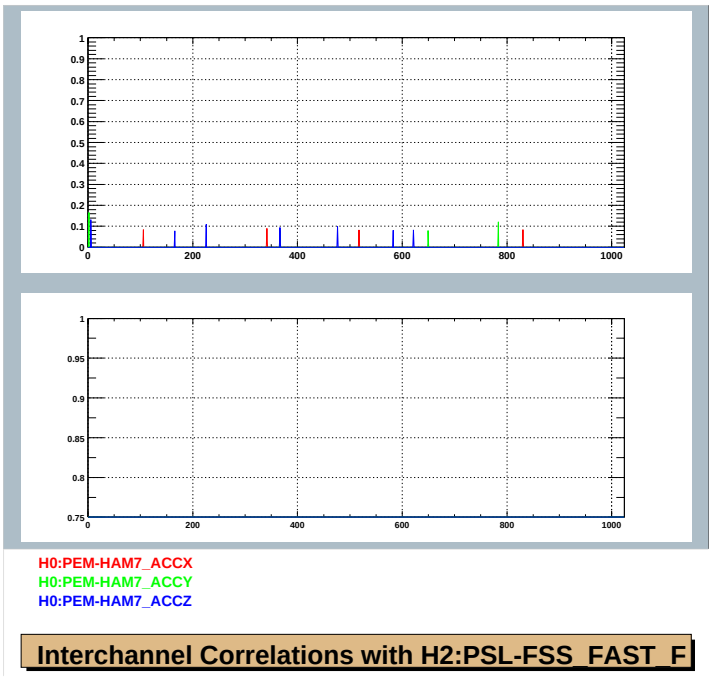

Figure 19: Correlations between laser fast frequency control signal, H2:PSL-FSS_FAST_F, and various accelerometers.

6 H2:PSL-ISS_ISERR_F

The intensity stabilization servo was correlated with the interferometer output H2:LSC-AS_Q. Low frequency correlations we coincident with 60 Hz and harmonics. Various correlations are found at higher frequencies. See Fig. 20.

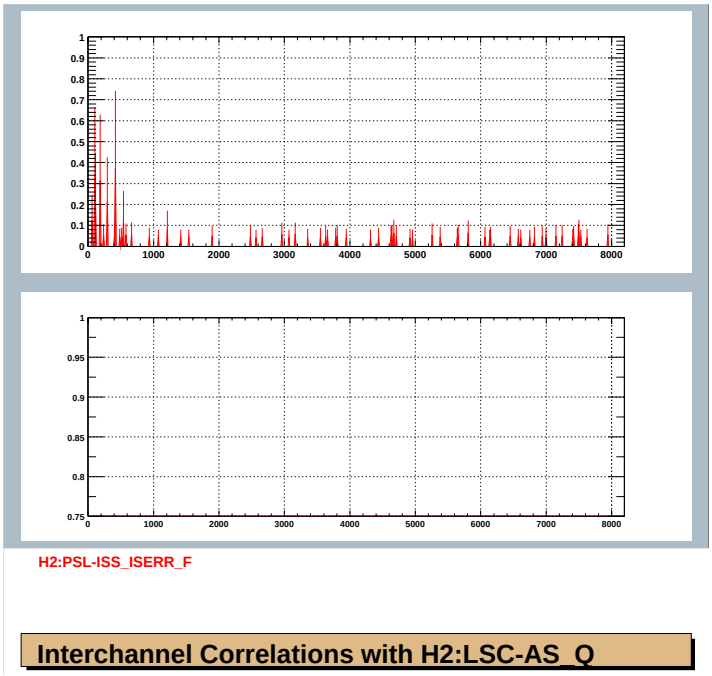

Figure 20: Correlations between H2:LSC-AS_Q and H2:PSL-ISS_ISERR_F. Low frequency correlations coincide with 60 Hz and harmonics.

Correlations were also calculated with various microphones (Fig. 21) and with accelerometers (Figs. 22 and 23). Many of these correlations correspond to 60 Hz and harmonics.

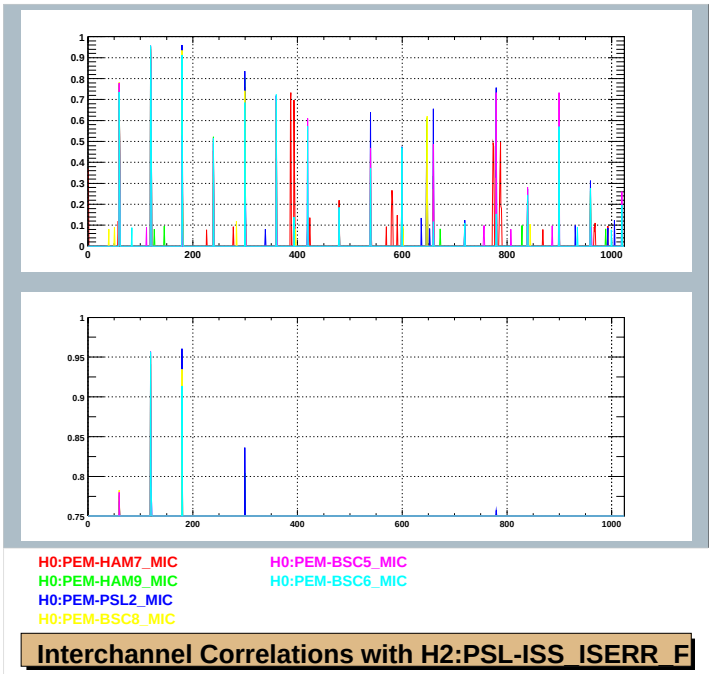

Figure 21: Correlation of intensity stabilization servo error signal H2:PSL-ISS_ISERR_F and various microphones.

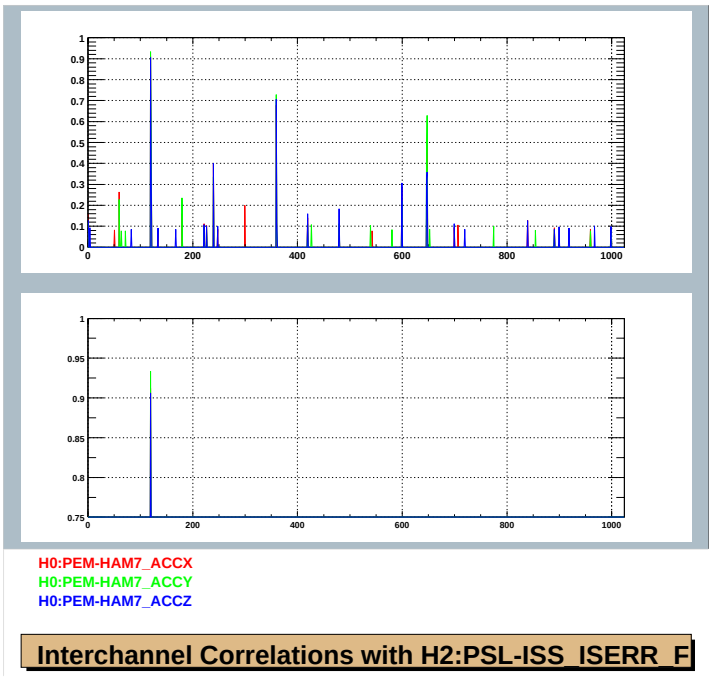

Figure 22: Correlation of intensity stabilization servo error signal H2:PSL-ISSER_F and HAM7 accelerometers.

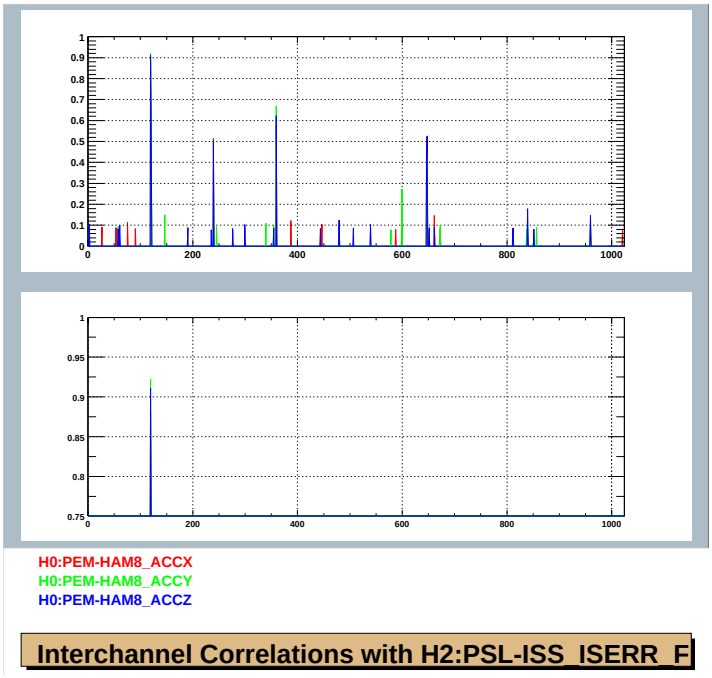

Figure 23: Intensity stabilization servo error signal H2:PSL-ISERR_F and HAM8 accelerometers.

7 H2:LSC-C(D)ARM_CTRL

The single arm control output H2:LSC-DARM_CTRL was correlated with some control signals, as seen in Fig. 24.

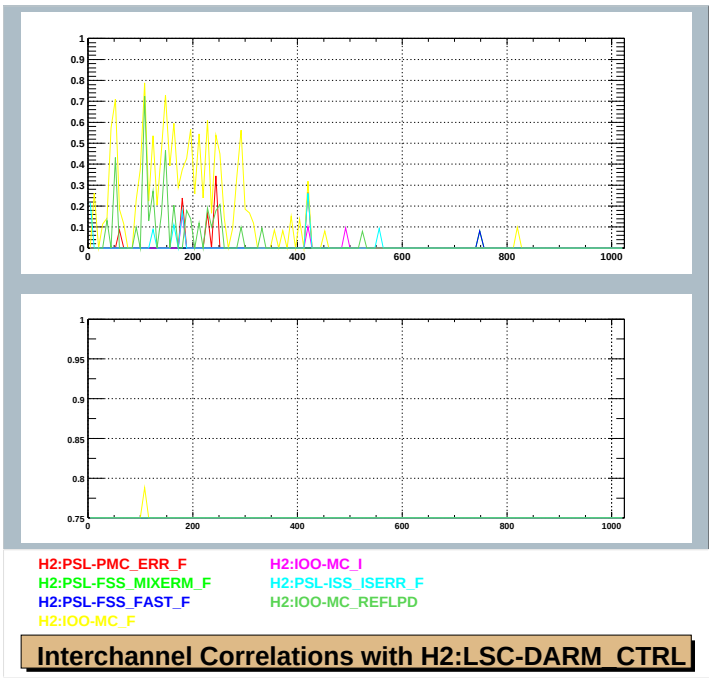

Figure 24: The interferometer arm control signal H2:LSC-DARM_CTRL is correlated with various control signals.

The single arm control output H2:LSC-CARM_CTRL was correlated with some control signals, as seen in Fig. 25.

The mode cleaner signal H2:IOO-MC_F is the dominant correlation for both H2:LSC-CARM_CTRL and H2:LSC-DARM_CTRL. H2:LSC-CARM_CTRL and H2:LSC-DARM_CTRL were also correlated with each other, Fig. 26.

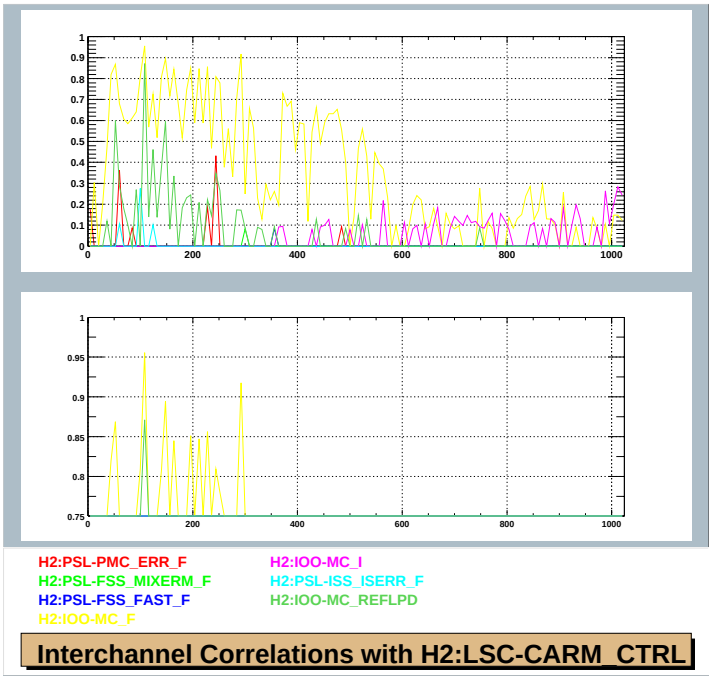

Figure 25: Interferometer arm control signal H2:LSC-CARM_CTRL is correlated with various other control signals.

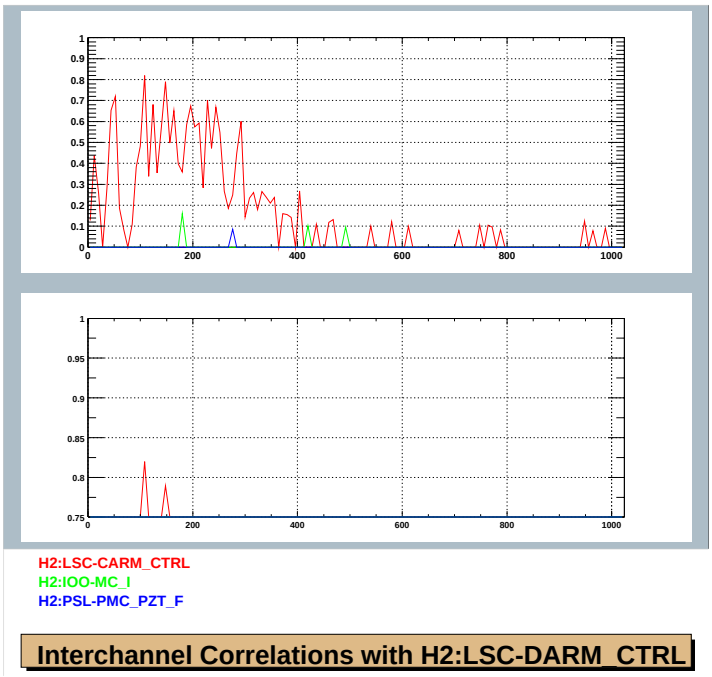

Figure 26: Correlation of the two interferometer arm control signals, H2:LSC_DARM_CTRL and H2:LSC_CARM_CTRL.

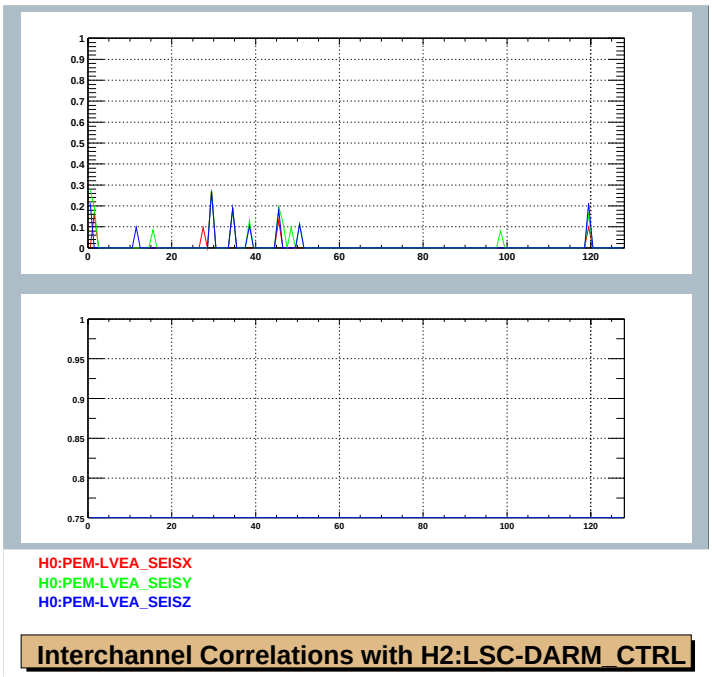

Figure 27: Correlation of interferometer arm control signal H2:LSC-DARM_CTRL and seismometers.

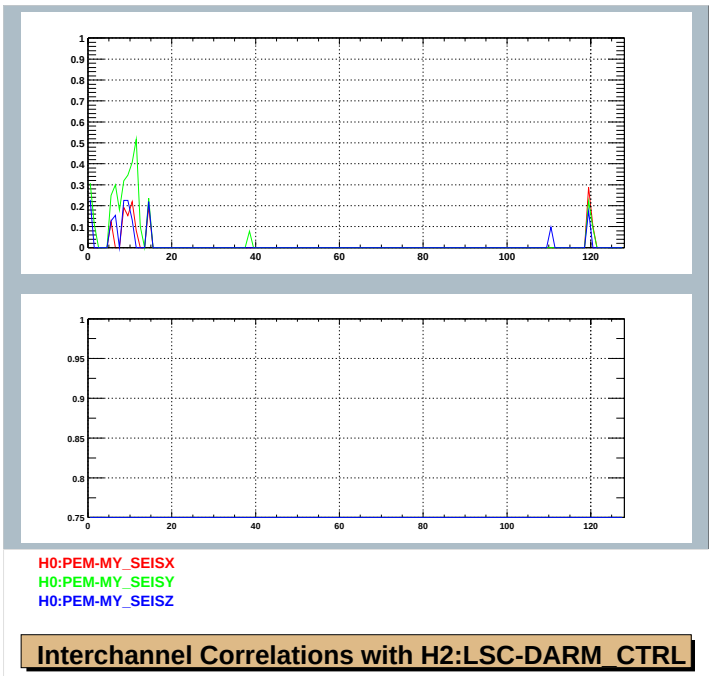

Figure 28: Correlation of interferometer arm control signal H2:LSC-DARM_CTRL and seismometers.

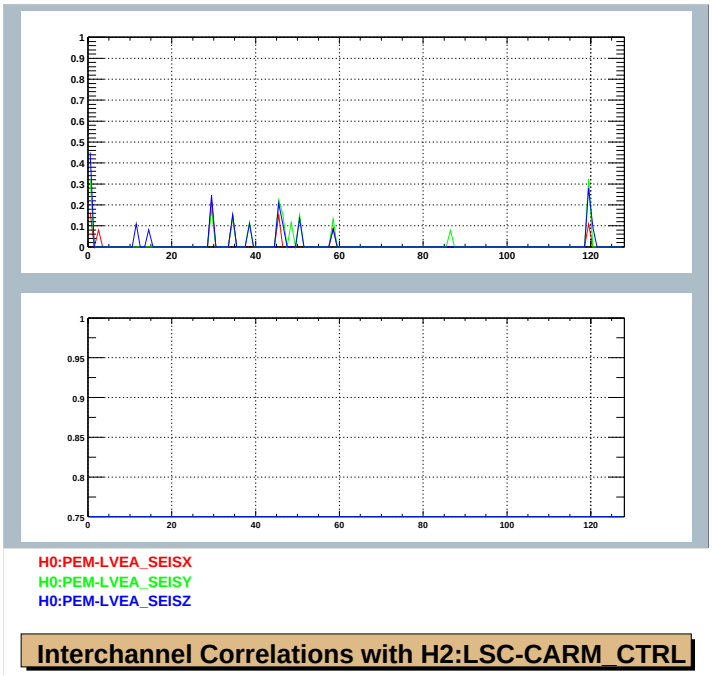

Figure 29: Interferometer arm control signal H2:LSC-CARM_CTRL with seismometers.

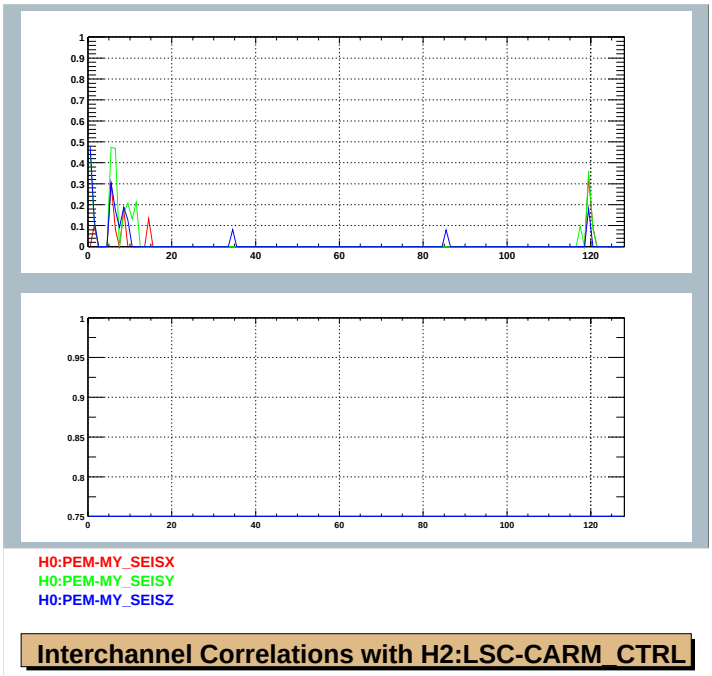

Figure 30: Interferometer arm control signal H2:LSC-CARM_CTRL with seismometers.

8 H2:LSC-MICH_CTRL

The Michelson interferometer control signal was correlated with various other control signals, Fig. 31. Once again the main correlation is from the mode cleaner.

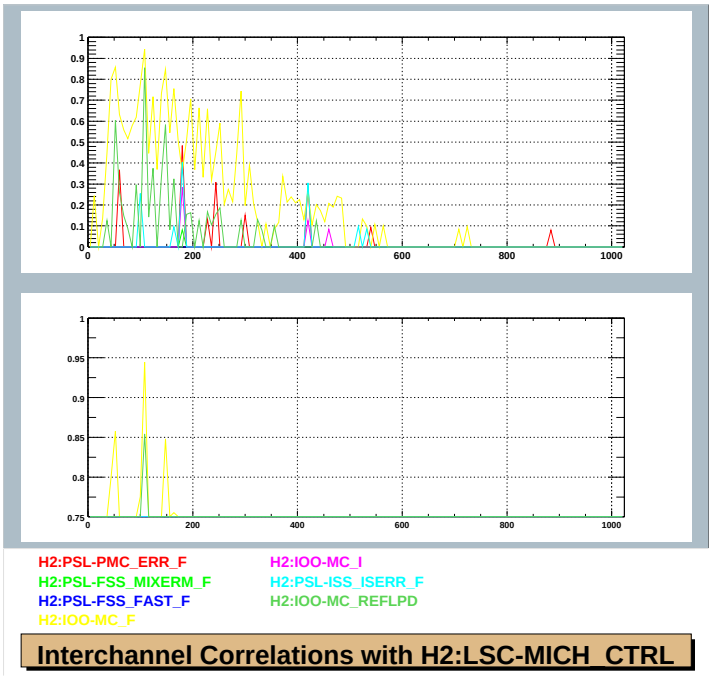

Figure 31: The Michelson interferometer control signal H2:LSC-MICH_CTRL with various control signals.

The correlations observed with the seismometers looks just like those for H2:LSC-CARM_CTRL and H2:LSC-DARM_CTRL; for example, see Fig. 32.

9 H2:LSC-REFL_I and H2:LSC-REFL_Q

There is broad correlation between H2:LSC-REFL_I and H2:LSC-AS_Q below 1 kHz; see Fig. 33.

Correlations of H2:LSC-REFL_I and H2:LSC-AS_Q can be seen at various ranges of frequencies, below 1 kHz, at 1.6 kHz, and 3.3 kHz. This is possibly consistent with results of the line noise group [3]; see their Figs. 22 and 23. Compare this with our Fig. 34.

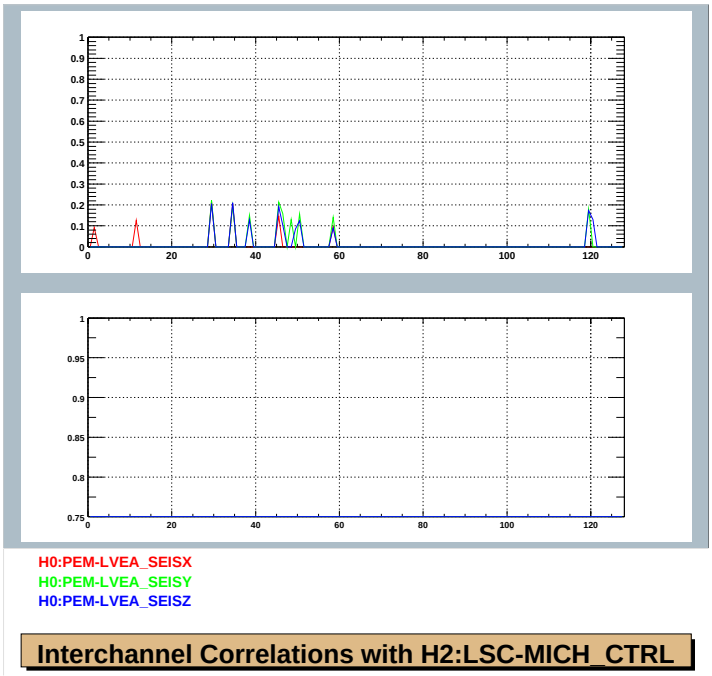

Figure 32: Michelson interferometer control signal H2:LSC-MICH_CTRL correlated with some seismometers.

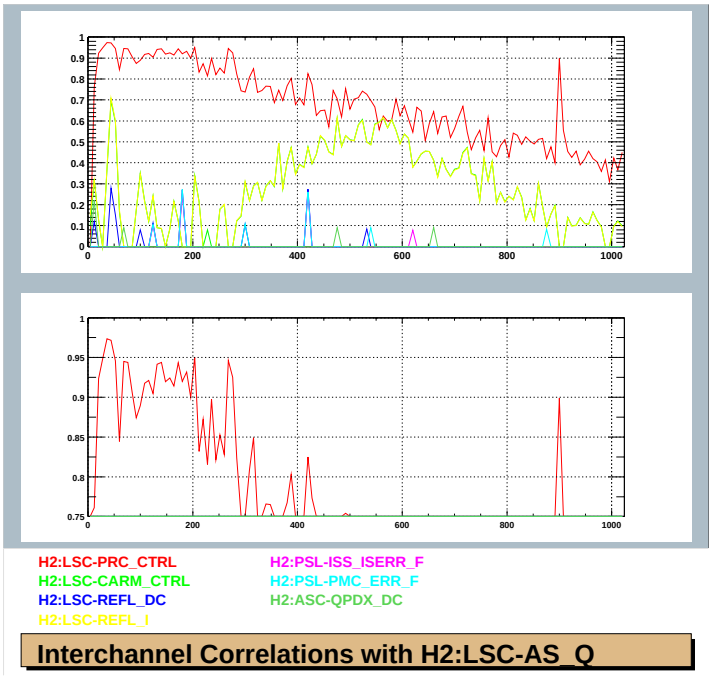

Figure 33: Correlation between H2:LSC-REFL_I and H2:LSC-AS_Q is strong below 1 kHz.

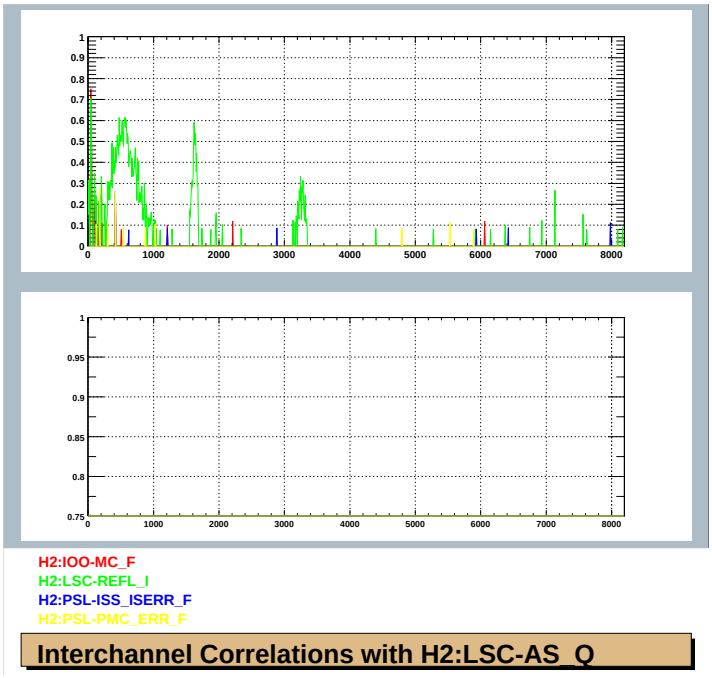

Figure 34: Correlations between H2:LSC-REFL_I and H2:LSC-AS_Q.

10 Bicoherence

In order to observe possible non-linear coupling between noise at differing frequencies we have just started to use higher order statistics. For instance, the bicoherence was used to try to observe correlated E2 H2:LSC-AS_Q noise at the different frequencies. See [4] for details of the technique. Fig. 35 was made with four seconds of data from H2:LSC-AS_Q. Some strong correlations between frequencies were observed below 100 Hz. It was informative to also observe the bicoherence at larger frequencies. In Fig. 36 we see correlations between low frequency nose ($<$ 100Hz) out to the higher frequencies. Note the relatively strong correlation around 750 Hz.

Steve Penn (U. Syracuse) is joining the correlation effort for analyzing the E3 data. The intent is to use a monitor that tests the gaussianity of a channel. This test calculates the bispectrum and the bicoherence. It then integrates the bicoherence over the unique region of the bispectrum. This integral obeys chi-squared distribution. If the channel is gaussian then the integral is zero. Thus one can use the chi-squared distribution to test the probability that the channel is gaussian. S. Penn is presently working on another monitor to try and display the bispectrum in real time. This would be a visual, qualitative monitor rather than performing a statistical test.

It was also very interesting to observe correlation between $\sim$50 Hz noise and that at $\sim$3.2 kHz. As noted before, the 3.2 kHz region seems to be a problematic area for interferometer noise [3]; see Fig. 37.

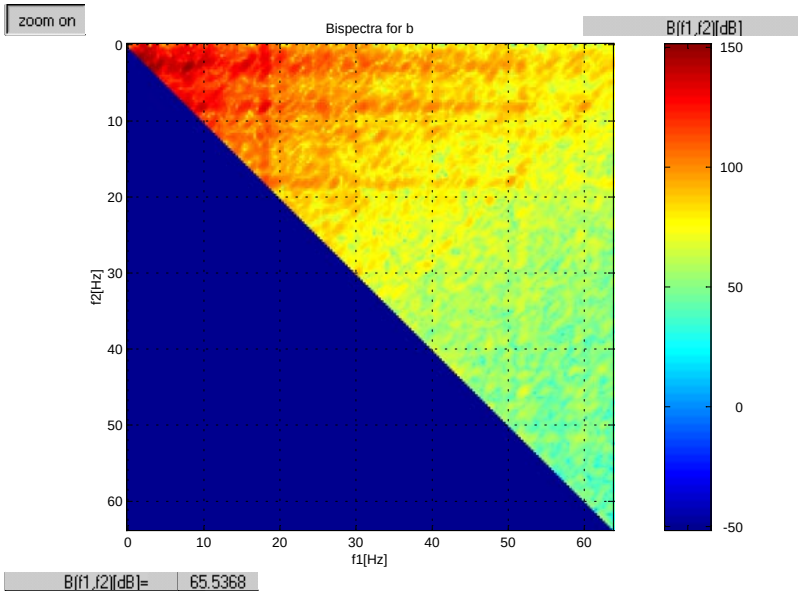

Figure 35: Bicoherence of H2:LSC-AS_Q up to 60 Hz

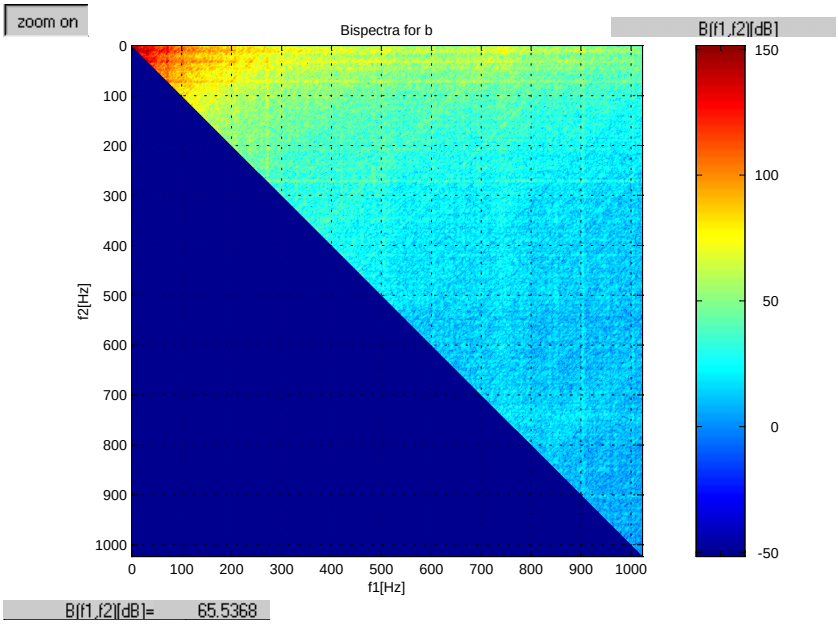

Figure 36: Bicoherence of H2:LSC-AS_Q up to 1 kHz

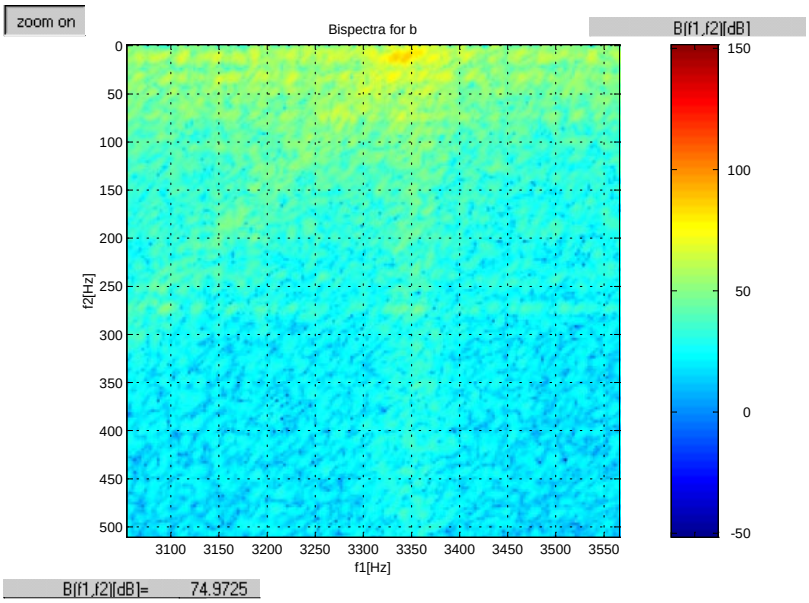

Figure 37: Correlation between ∼50 Hz noise and that at ∼3.2 kHz

This work was supported by National Science Foundation grant PHY-0071327.

References

[1] A. Ottewill, `http://blue.ligo-wa.caltech.edu/gds/dmt/Monitors/DEnvCorr`

[2] B. Allen, W. Hua and A. Ottewill, gr-qc/9909083

[3] R. Coldwell, R. Flaminio, S. Klimenko, A. Sintes, B. Whiting, *Narrow Resonances in the E2 Data*, 2001.

[4] D. Petrovic, A. Lazzarini, *Use of Higher Order Statistics [HOS} to Detect and to Characterize Non-Gaussian Noise*, LIGO-T990084-00-E, 1999.